

Article

An Analysis of the Weldability of Ductile Cast Iron Using Inconel 625 for the Root Weld and Electrodes Coated in 97.6% Nickel for the Filler Welds

Francisco-Javier Cárcel-Carrasco *, Miguel-Angel Pérez-Puig, Manuel Pascual-Guillamón and Rafael Pascual-Martínez

ITM, Universitat Politècnica de València, Valencia 46022, Spain; mipepui@mcm.upv.es (M.-A.P.-P.); mpascual@mcm.upv.es (M.P.-G.); rapasmar@hotmail.com (R.P.-M.)

* Correspondence: fracarc1@csa.upv.es; Tel.: +34-963-87-7000; Fax: +34-963-87-9459

Academic Editor: Giuseppe Casalino

Received: 26 July 2016; Accepted: 14 November 2016; Published: 18 November 2016

Abstract: This article examines the weldability of ductile cast iron when the root weld is applied with a tungsten inert gas (TIG) welding process employing an Inconel 625 source rod, and when the filler welds are applied with electrodes coated with 97.6% Ni. The welds were performed on ductile cast iron specimen test plates sized 300 mm × 90 mm × 10 mm with edges tapered at angles of 60°. The plates were subjected to two heat treatments. This article analyzes the influence on weldability of the various types of electrodes and the effect of preheat treatments. Finally, a microstructure analysis is made of the material next to the weld in the metal-weld interface and in the weld itself. The microstructure produced is correlated with the strength of the welds. We treat an alloy with 97.6% Ni, which prevents the formation of carbides. With a heat treatment at 900 °C and 97.6% Ni, there is a dissolution of all carbides, forming nodules in ferritic matrix graphite.

Keywords: weldability; pre-heating; ductile cast iron; microstructure; root pass

1. Introduction

Castings such as steel are basically alloys of iron, carbon, and silicon that favor the formation of graphite, and carbon content may vary between 2% and 6.67%. Carbon percentages of up to about 4% are often used commercially because a large percentage of carbon may affect brittleness. Alloys obtained in casting processes are generally neither ductile nor malleable. The EN 1563 normative defines ductile cast iron as a “casted material based on iron, carbon and silicon, and in which carbon is primarily in the form of spheroidal particles”.

Classification depends on the metallographic structure and the percentages of carbon, alloy elements, and impurities. The poor mechanical properties of some castings are due to the presence of graphite flakes [1] that produce discontinuities in the matrix and so lead to the presence of stress concentrators.

These alloys have a high carbon content that makes them difficult to weld because of the formation of martensite and brittle iron carbides during the cooling of the joining process [1,2]. Due to this, welding on cast iron generally involves repair operations and not joining casting between them, although this last operation can be performed following some precautions [3]. These precautions are mainly oriented to the selection of the filler metal [3–5] and the reduction of the cooling rate of the weld in order to reduce martensitic transformations and carbide precipitations, which would with ease lead to the cracking of the joint.

Adding pure magnesium, magnesium ferrosilicon, or magnesium-nickel to an alloy encourages the formation of graphite nodules that improve the characteristics of the casting by combining the mechanical strength, toughness, and ductility of steel with the moldability of gray iron.

The process of welding the filler partially determines its mechanical properties. The result is also influenced by preheating treatments and cooling rates. A subsequent normalization process also improves the properties.

This study examined the weldability of ductile cast iron (in two circumstances: before and after an annealing post-treatment to dissolve any hard precipitates and restore the microstructure of the heat affected zone) when the root weld is applied with a tungsten inert gas (TIG) welding process employing an Inconel 625 source rod, and when the filler welds are applied with electrodes coated with 97.6% Ni.

2. Materials and Methods

2.1. Composition and Mechanical Characteristics of the Castings Used

Graphite appears as nodules in ductile cast iron because of the presence of small amounts of magnesium [1] retained by the iron and distributed evenly throughout the matrix. Magnesium eliminates the discontinuity caused by the graphite grain in gray cast iron and produces significant improvements in the mechanical characteristics in comparison with gray iron. The chemical composition of ductile cast iron expressed in percentages can be seen in Table 1. The mechanical properties of the castings considered in this study are shown in Table 2.

Table 1. Alloying elements of ductile cast iron.

Cast	%C	%Si	%Mn	%S	%P	%Ni	%Cu	%Cr	%Mo	%Mg
Ductile	3.71	2.54	0.04	<0.01	0.02	0.02	0.026	0.03	<0.01	0.03

Table 2. Mechanical properties of ductile cast iron.

Mechanical Characteristics	Values
Tensile strength (MPa)	370
Yield strength (MPa)	320
Elongation (%)	6
Elastic modulus (MPa)	160,000
Brinell hardness	190
Fatigue limit (MPa)	280

EN 1563 specifies the characteristics for ductile iron, while EN 1561 specifies the characteristics for gray cast iron. The process of welding the specimens of ductile iron was made using the following techniques: tungsten inert gas (TIG) welding and manual arc welding with coated electrodes (SMAW).

TIG welding is one of the most common techniques for welding elements whose thickness is less than 8 mm. The process is recommended for root welding pieces of even greater thickness to ensure sufficient penetration in the bonding processes, and for welding ductile iron castings that require prior preparation. The welds were made on ductile cast iron plates described in Table 2 using ER Inconel 625 source rods after preheating the test specimens. Various largely irrelevant distortions may have been present in the test plates.

Arc welding is one of the techniques most used for welding ductile cast iron, and filler material was added with two SMAW passes over the TIG root weld [6]. The test plates may have revealed largely irrelevant distortions after being preheated. The filler weld was made using 97.6% Ni electrodes in order to minimize carbide formation as well as improving the service conditions. The weld was carried out on a series of test plates that were pre-heated to 350 °C. Once the welds were finished, some

of the plates were air-cooled, while others were immediately annealed at 900 °C in order to observe the different metallurgical behavior produced by these treatments [7].

The specimen test plates were produced in a sand casting process and originally measured 300 mm × 95 mm × 11 mm. They were subsequently milled to 300 mm × 95 mm × 10 mm (coupon). The edges were prepared for electric welding with a covered electrode by cutting a 30° chamfer so that with proper spacing a perfect union could be achieved along the entire thickness of both plates. This preparation was made using an adjustable band saw [6].

The electrodes used for the welding were selected to obtain optimum results [8] in terms of the mechanical properties in the process of joining the castings. Compositions are shown below in Table 3.

Table 3. Electrodes used for ductile iron welds.

Electrode	Composition	
	Element	%
Inconel 625	Si	0.5
	Mn	0.5
	Ni	58
	Cr	20–25
	Nb	3.5
	Ta	4.5
	Mo	8–10
	Fe	Other
Ni 97.6%	C	<0.1
	Si	<0.4
	Mn	0.20
	Ni	97.61
	Fe	Other

2.2. Welding Processes

TIG root welding using Inconel 625 source material (1.5 mm in diameter) was carried out using a continuous welding current of between 120 and 130 A, straight polarity, and an argon flow of 12 L/min. The welding seam was performed in a single circular pass in a horizontal right to left motion and an inclination angle of the tungsten electrode of between 70° and 80° when moving forward, and an angle of about 20° above horizontal for the source rod. The plate was preheated to 350 °C before welding. Shielded metal arc welding (SMAW) was performed with direct current and reverse polarity (due to the basic character of the coating) and using 140 A and a 3.2 mm electrode diameter that was previously heated at 90° for 24 h at 100 °C (to improve fluidity and hydrogen inclusion and thereby prevent cracking). The weld was carried out with two filler passes from left to right horizontally with an electrode angle of inclination of approximately 60°.

Because of the difficulty in welding the castings and to avoid fractures due to the stresses generated during cooling, we preheated the castings to 350 °C before welding, lightened the bead in sections separated by more than 40 mm, and hammered the plates vigorously. Various problems arose due to the breakdown of the electrodes, excessive intensity as the weld progressed, difficulties in removing the coating, and a lack of fluidity.

To solve these problems, a suitable preparation was made that left a separation adequate to prevent sticker breaks [5] and ensure good penetration. It was also decided to change the electrodes when one-half was consumed and thus avoid deterioration by decomposition (thereby preventing the formation of porosities or internal inclusions). The electrodes were reused once cold.

Due to the heating of the material, a decreasing amount of intensity was required; however, if intensity was reduced too much, then sticker breaks may have formed. Changing the electrode before it was consumed provided sufficient cooling time for the material without having to reduce

intensity. Moreover, it was possible to vary the speed of the welding movement to prevent filler source burning.

The test plates were initially root welded using Inconel and then welded with coated electrodes for the filler. The plates (once adequately prepared) were welded after a preheat at 350 °C in order to reduce the tensions, slow the cooling, increase the fluidity of the welds (preventing pores forming and cracks in the bead), and thus facilitate a reduction in intensity to about 120–130 A. Some of the test plates were annealed at 900 °C after welding and cooled in the furnace.

The corrosive liquid used to make the microstructure of ferrite, white iron, and martensite clearer and to improve the quality of photographs was called “Nital 3”.

3. Results

We measured the Vickers micro hardness (HV), yield strength, tensile strength, and elongation as the average of tests using five different sizes.

The HV micro hardness was measured with 300 g loads for 10 s with a diamond point at 136°. Measurements were taken in the zone adjacent to the weld, in the metal-weld interface, and the weld zone (a total of nine measurements) in accordance with UNE-EN 876. The mechanical properties are shown in Table 4 (the micro hardness was made in areas close to Figures 3 and 6). The tensile tests to determine the mechanical properties were carried out in accordance with UNE-EN 10002-1 for tensile tests at room temperature with a universal testing machine and a maximum force of 10 t. The results are shown in Table 4.

Table 4. Mechanical properties of the ductile iron welds.

Welding	Rod	S (MPa)	YS (MPa)	A%	H _V Interface	H _V Welding	H _V HAZ
Pre-heating 350 °C and air cooling	Inconel 625 root Ni 97.6% filler	320	310	5.5	730 490	510 191	295
Pre-heating 350 °C and annealed at 900 °C	Inconel 625 root Ni 97.6% filler	300	285	7	610 230	400 160	210

Figures 1–8 show the microstructures produced by the different types of welds. Figure 9 shows the different types of fractures that occurred during standard testing [9,10].

4. Analysis of Results and Discussion

Micrographs of TIG root welds (made with Inconel 625) of the ductile iron test plate following a preheat treatment at 350 °C (but without subsequent annealing treatment) (Figure 1) reveal in the interface structures formed by traces of white iron in which most of the graphite has combined to form cementite. Very small and uniformly distributed spherulites can also be seen. The rate of cooling also produced martensite precipitates, a partial consequence of the effect of Ni on the dissolution of the carbides being counterbalanced by the effect of Cr as a stabilizer. The Vickers hardness was 460, mostly in areas where the carbides precipitated. The consequence was the beginnings and expansion of a brittle fracture in the zone of the interface. The structure can be defined as a martensite white iron matrix.

The micrograph shows the manual weld of ductile cast iron using an electrode coated with 97.6% Ni (Figure 2) made on top of an Inconel root weld. The image reveals a structure in which traces of white iron have significantly diminished, resulting in a higher concentration of nodules of uniformly distributed graphite that are larger than those shown in the previous micrograph. This is largely due to the Ni content of the coated filler electrode, largely preventing the formation of carbides in the dilution zone; however, it is also possible to see martensite precipitate in the austenitic matrix (in which the Vickers hardness is 700 as a result of the rapid cooling of the weld). The fracture has extended in the interface zone, which has become brittle because of the cooling rate.

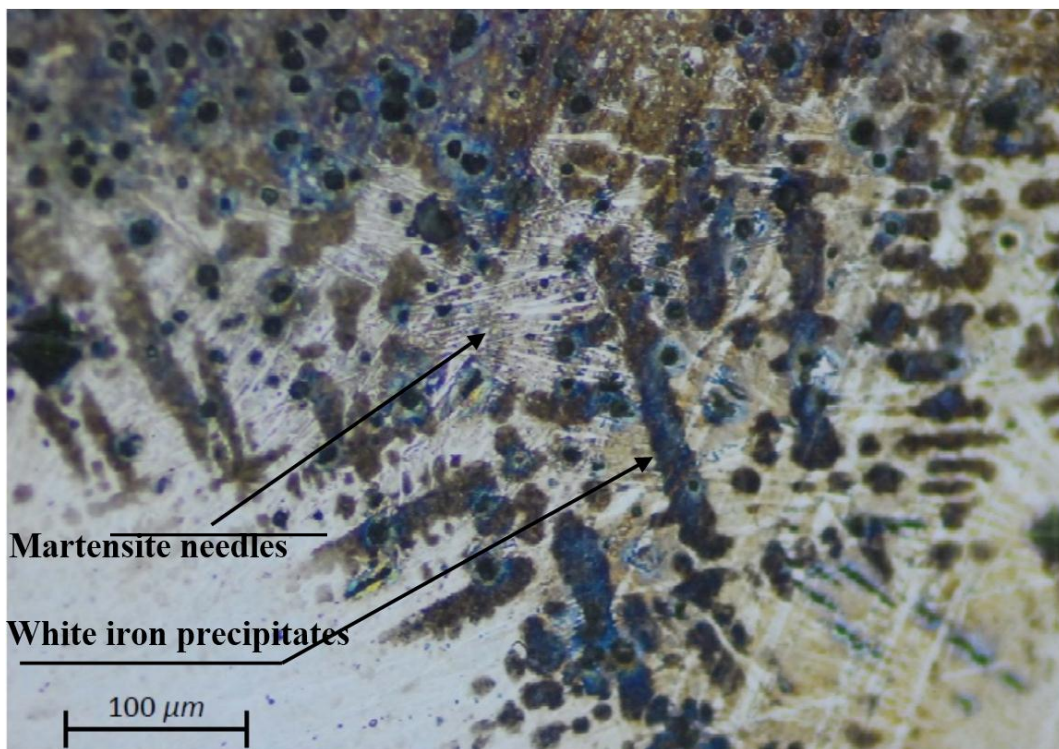


Figure 1. Micrograph of the ductile iron tungsten inert gas (TIG) root weld using Inconel 625 and without subsequent annealing.

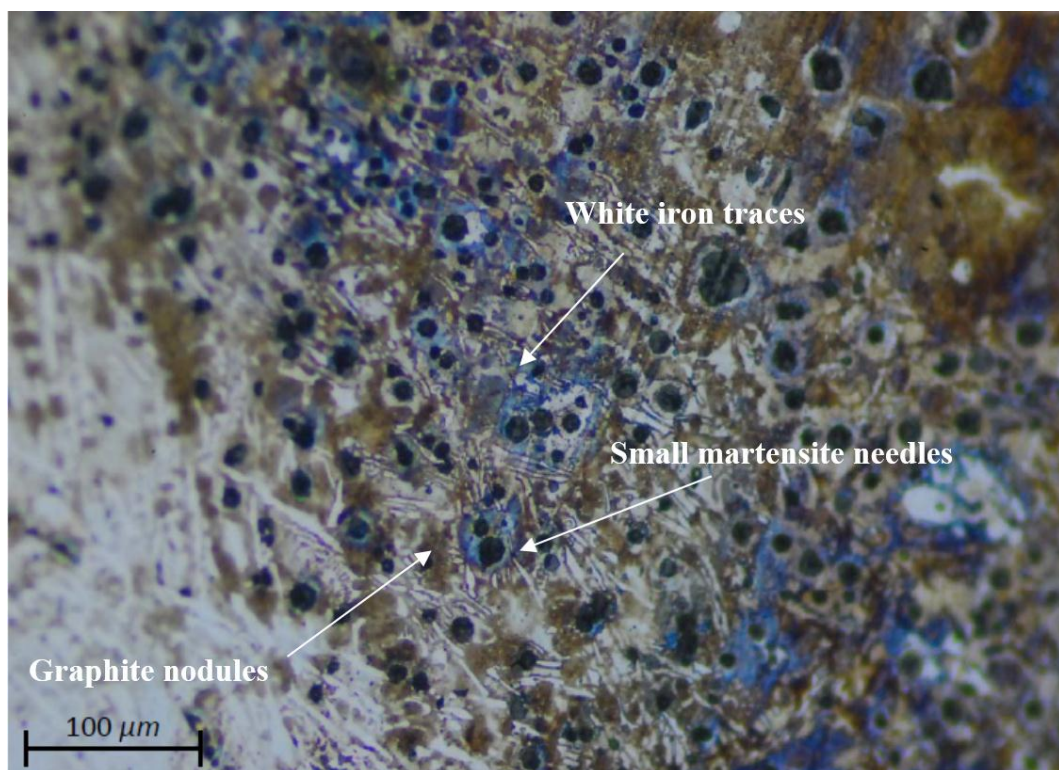


Figure 2. Micrograph of ductile iron weld using 97.6% Ni coated electrode on an Inconel root weld without heat treatment.

In a micrograph of a filler weld made with a 97.6% Ni electrode with a maximum dilution of the base material and preheating to 350 °C followed by air cooling (Figure 3), three zones can be distinguished: weld, base material, and interface [11,12].

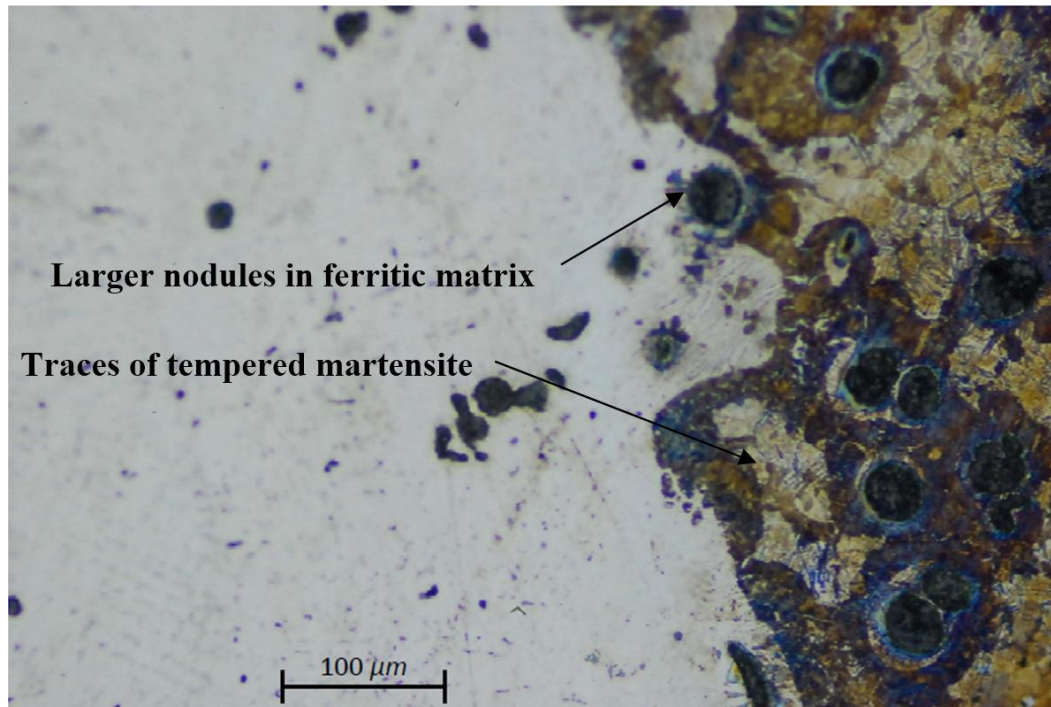


Figure 3. Micrograph of a weld performed with a 97.6% Ni electrode on a ductile iron casting with heat treatment at 350 °C and air cooling.

Ferritic-pearlitic ductile iron can be seen in the vicinity of the base material near the weld. This material does not provide high levels of hardness (360 HV) and becomes more similar to the base material in hardness as we move away from the area affected by heat. At the interface of the weld, we can see martensite precipitates tempered in a ferrite matrix (as a result of the Ni content in the filler metal) with slight traces of cementite and graphite nodules (smaller than those in the casting) that are uniformly distributed over the entire zone. The hardness produced at this stage is greater than the base metal. In the region of the weld, the graphite appears as nodules that are smaller than those in the interface and evenly distributed across the weld. The hardness is lesser than that obtained in the interface, and fractures occur in the weld zone near the brittle interface.

In the micrograph of the base material (Figure 4), structural formations of material near the weld and at the boundary of the heat affected zone can be seen. These ferriticpearlitic structures contain uniform nodules that are larger than those visible in the micrographs of the interface between the filler material and the ductile iron. These structures are uniformly distributed and similar to the structures of the material from which the test plates are made albeit generally harder.

The micrograph (Figure 5) shows the formation of nodules in the weld made with filler material applied with a 97.6% Ni electrode where a uniform distribution of ferritic material and traces of retained austenite can be found with sizes smaller than those found on the base material. A distribution similar to that shown above can be found in the structure on the Inconel 625 filler material used in the root weld.

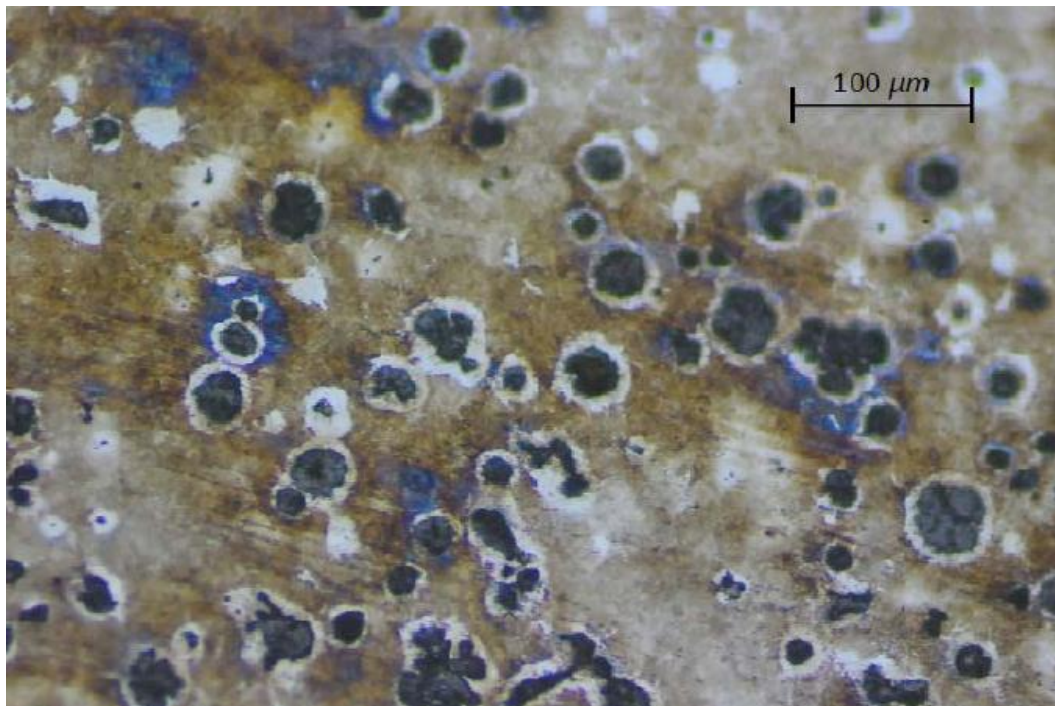


Figure 4. Micrograph of the structure produced on the base material at the edge of the heat affected zone.

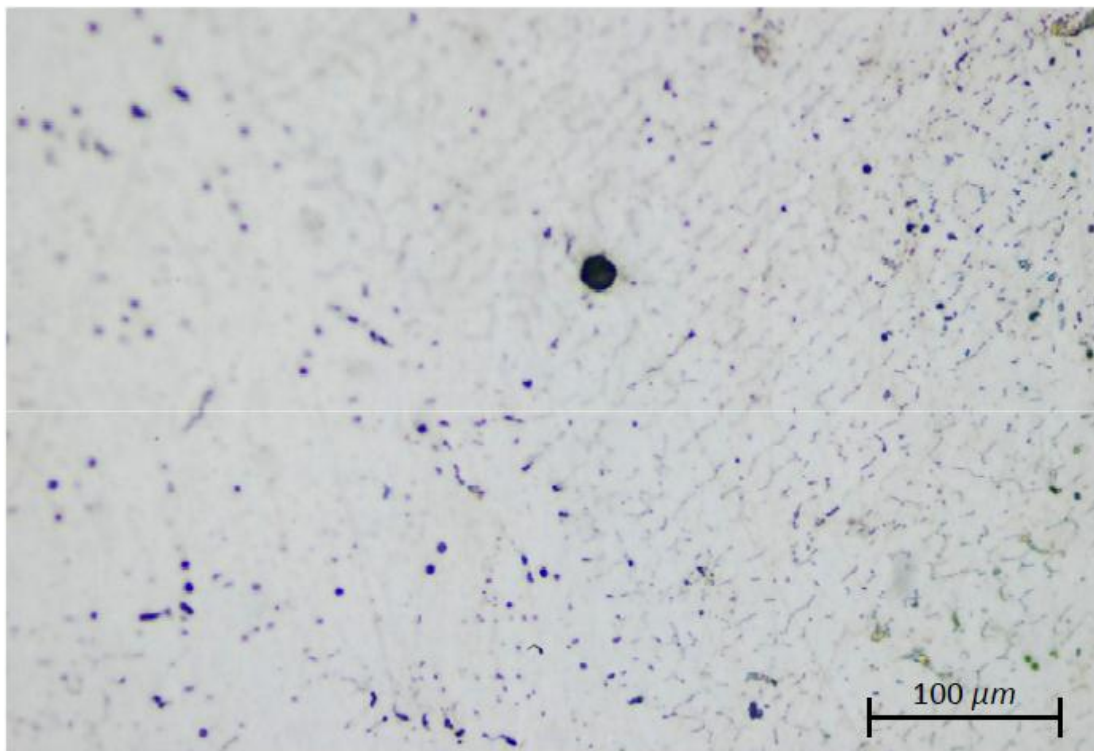


Figure 5. Micrograph of the material deposited on the ductile iron weld.

A transformation of the ferrite structure in the interface near the metal base can be seen in the micrograph of the weld obtained with a 97.6% Ni coated electrode on ductile iron in the filler zone on the second pass—and with subsequent heat treatment at 900 °C (Figure 6). The transformation is a consequence of thermal annealing and the increased Ni in the filler. This implies a considerable reduction in the strength of the material and an increase in the elongation at fracture with respect to the filler metal (in which nodules that are smaller than those in the interface are precipitated) [13,14] and the base metal where the hardness is lesser than samples made without preheating. The fracture is more ductile than in the previous cases and usually occurs in the cast zone near the interface [15].

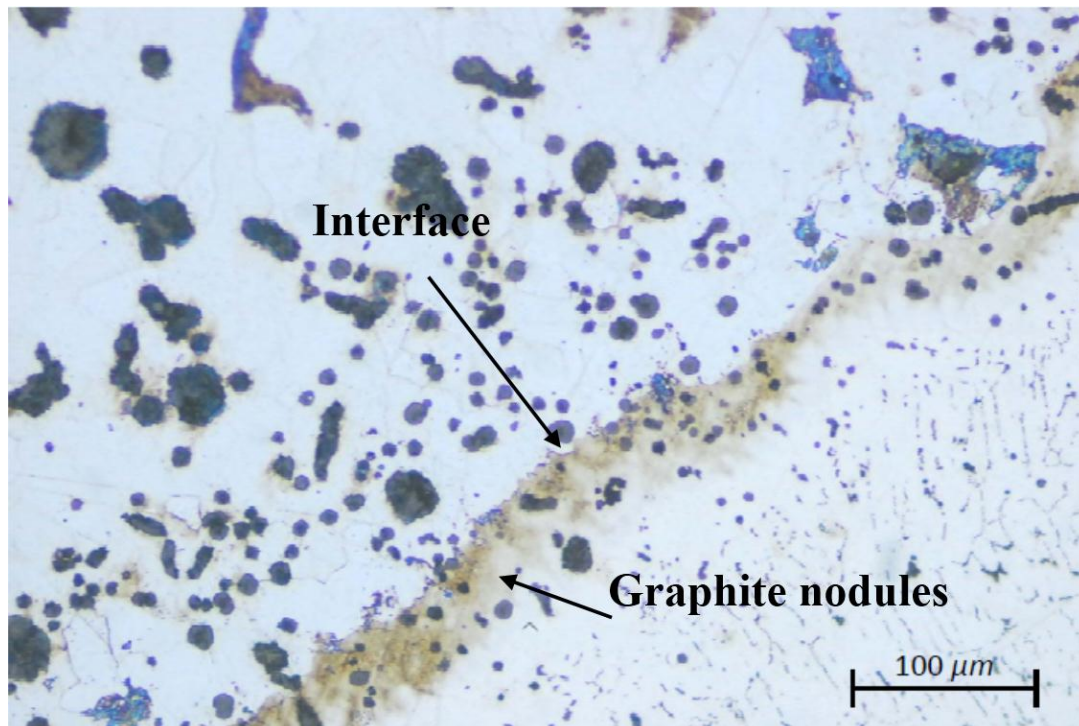


Figure 6. Micrograph of the filler zone in a ductile iron weld using a 97.6% Ni coated electrode with subsequent thermal annealing at 900 °C.

In the micrograph of the interface of the ductile iron TIG root weld made with an Inconel 625 electrode and preheating to 350 °C and with subsequent annealing treatment at 900 °C (Figure 7), it can be seen that, despite the heat treatment, small traces of white iron in a martensitic matrix remain undissolved. Vickers hardness levels of 600 are produced—this being below the levels obtained using air cooling because the Cr content in the Inconel has retained part of the carbides formed in the weld. The illustration shows a higher amount of graphite nodules that are smaller than those found in the air-cooled base material. The fracture was brittle in this zone and started at the interface.

The emergence of iron carbide (cementite) is influenced by the speed of cooling metastable, while Ni (nickel) is a gammageno element, which prevents the formation of carbides, given the amount of carbon present in the composition smelting, and added to the fast cooling of the welding speed, resulting in the precipitation of carbides of iron that can later be dissolved with annealing heat treatments.

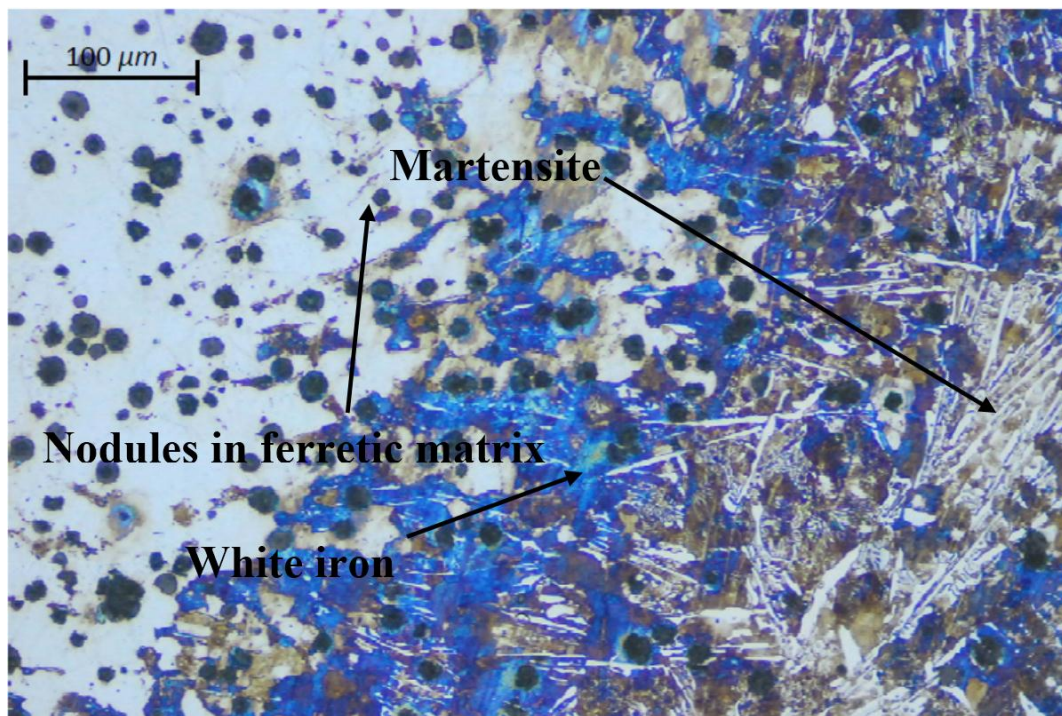


Figure 7. Micrograph of a root weld in ductile iron made with Inconel 625 and subsequent heat treatment at 900 °C.

The left part of the micrograph (Figure 8) shows that, after the annealing step, the ductile iron passed from ferritic-pearlitic ductile iron to ferritic iron with slightly larger and uniformly distributed nodules. The hardness is less than the original casting but with greater elongation at fracture. The micrograph on the right shows a uniform distribution of spherulites in the weld filler metal, and these are smaller in the ferrite matrix as a consequence of the Ni content and the furnace cooling rate.

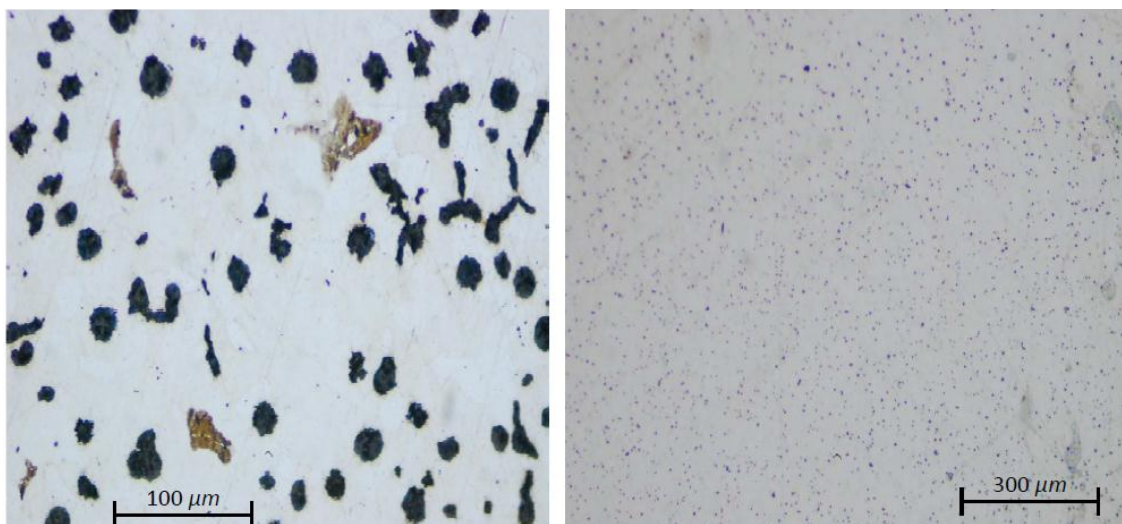


Figure 8. Micrographs of ductile iron showing the distribution of the nodules on the weld after annealing at 900 °C.

Manual arc welding with an electrode of 97.6% Ni is straightforward, the weld not being excessively fluid and high levels of carbide formation not occurring. Hardness is considerably less than that obtained in the root weld made with an Inconel source rod, although mechanical properties are acceptable and there is greater elongation at fracture. Micrographs show that an annealing treatment caused the martensitic structures to disappear and dissolved the traces of white iron producing a structure of nodular graphite on top of the ferrite matrix with an increased level of deformability [16–18].

Fractures according to the type of weld are shown in Figure 9.

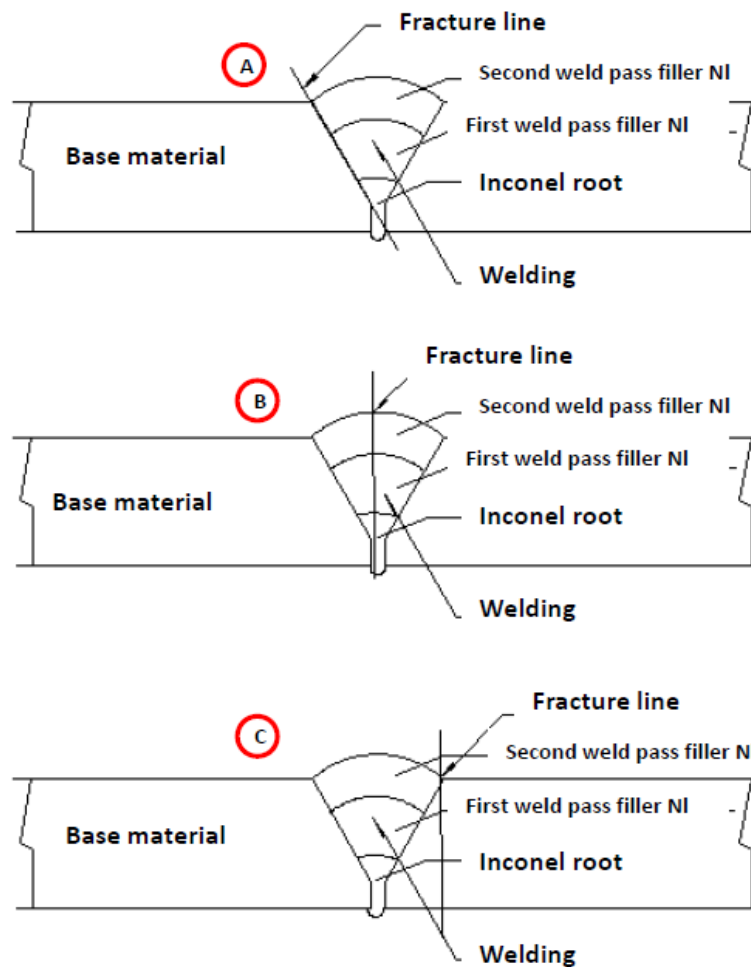


Figure 9. Zones of metallographic observation: (A) weld base metal base interface, (B) weld bead, (C) base metal.

The scanning electron microscopy (SEM) in Figure 10 shows the interface zone in the root weld applied with Inconel 625 but without heat treatment. Figure 11 shows the filler weld made with two passes of a 97.6% Ni coated electrode without treatment and the corresponding spectra. The spectrum in Figure 10 shows a high amount of chromium in the weld interface and the root weld where an Inconel 625 electrode was used—which influenced the formation of carbide precipitates that give rise to traces of white iron. The effect was to increase hardness and counteract the effect of Ni, as can be observed in the micrograph obtained for this zone in Figure 1. Another effect is the production of the beginnings of brittle fractures and a progressive growth of fractures in response to traction and bending.

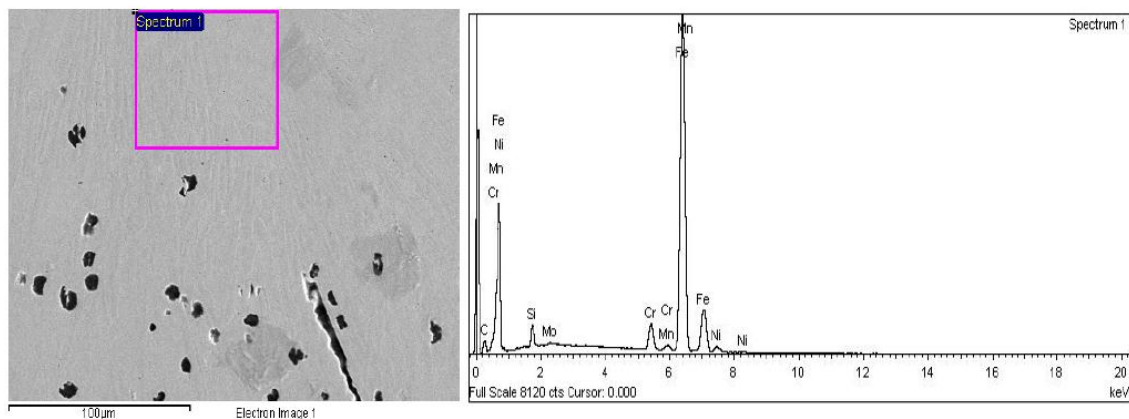


Figure 10. A SEM image and micrograph of the interface zone in a root weld without heat treatment and where a high amount of Cr can be observed in zones welded with Inconel.

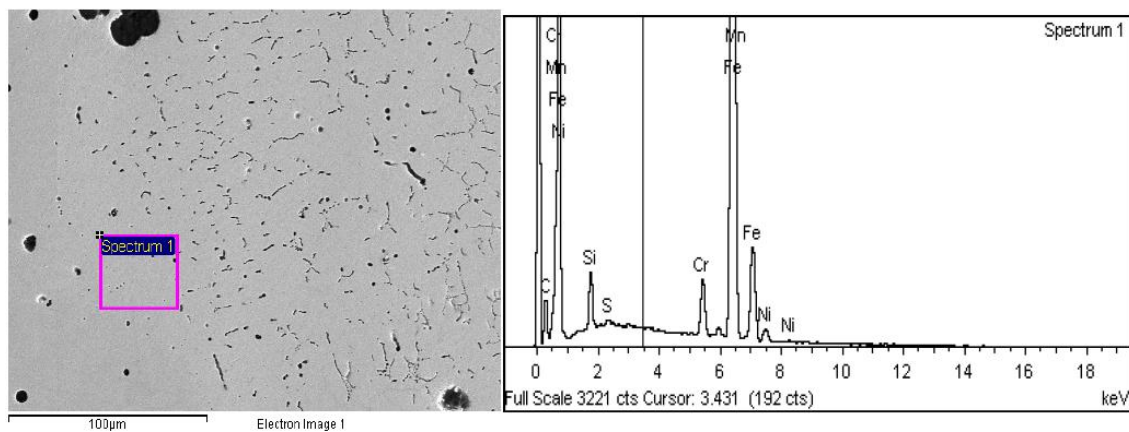


Figure 11. SEM and micrograph of the weld interface with filler applied using a 97% Ni electrode without subsequent heat treatment. Note the low Cr content.

The spectrum shown in Figure 11 corresponds to the interface of the first filler pass (97.6% Ni electrode) on the root pass weld (made using an Inconel 625 electrode). A remarkable decrease in the Cr content can be observed in the spectrum, causing a substantial decrease in traces of white iron and a greater influence of Ni on the structure (causing a decrease in hardness). A fracture initiated by bending and traction expands through the interface zone—as can be seen in the corresponding optical micrograph shown in Figure 2.

The SEM images in Figure 12 basically show the interface zone of the weld applied in the second filler pass with a 97.6% Ni electrode over the weld applied in the first pass (97.6% Ni) with subsequent annealing. Figure 13 shows the root weld on the same plate applied with Inconel 625 and annealed at 900 °C and the corresponding spectra.

The spectrum shown in Figure 12 corresponds to the second pass of the filler electrode (97.6% Ni) and annealing treatment at 900 °C with furnace cooling. We can observe a virtual absence of Cr, which directly influences the structure of the welding interface: dissolving the carbides and producing an absence of white cast iron and a substantial decrease in hardness. The result is a greater elongation at fracture. The graphite is precipitated in a fully nodular form, and the ferritic matrix can be seen in the optic micrograph in Figure 6. Tensile and bending fracture occurs in this zone near to the base material.

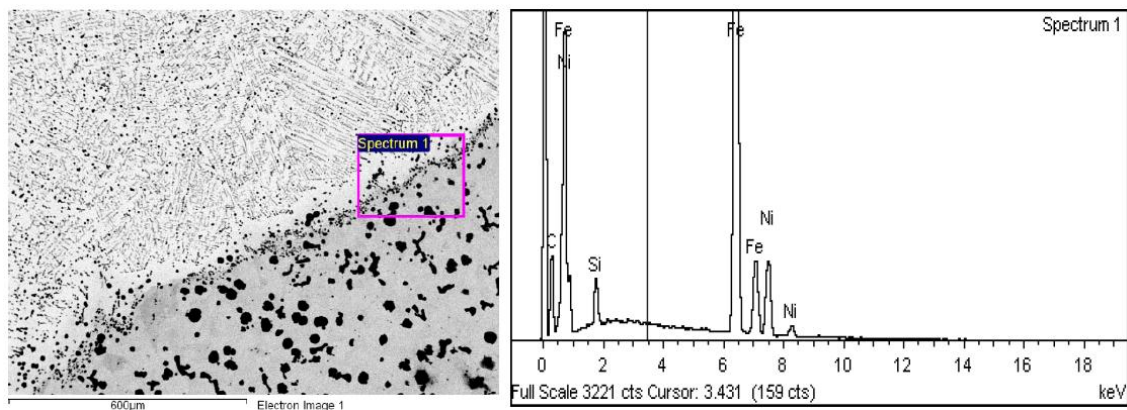


Figure 12. This figure shows micrographic and spectrum images of the filler weld interface of the top pass (electrode 97.6% Ni) and with a heat treatment at 900 °C. A higher content of free carbon is observed due to the dissolution of the white iron traces, while Cr is barely detectable (meaning greater ductility and less hardness).

The spectrum shown in Figure 13 corresponds to the interface of the root weld applied with an Inconel 625 rod and an annealing treatment at 900 °C and furnace cooling. The spectrum shows a decrease in Cr that is less pronounced than in the specimen with no heat treatment. The result is a partial reduction in carbides as a consequence of incomplete dissolution through heating and the speed of furnace cooling. As a consequence, there is a reduction in hardness at the interface although it remains very hard (as can be seen in the optical micrograph in Figure 7). The result is a substantial increase in strain capacity, although the fracture is brittle and starts in the root zone.

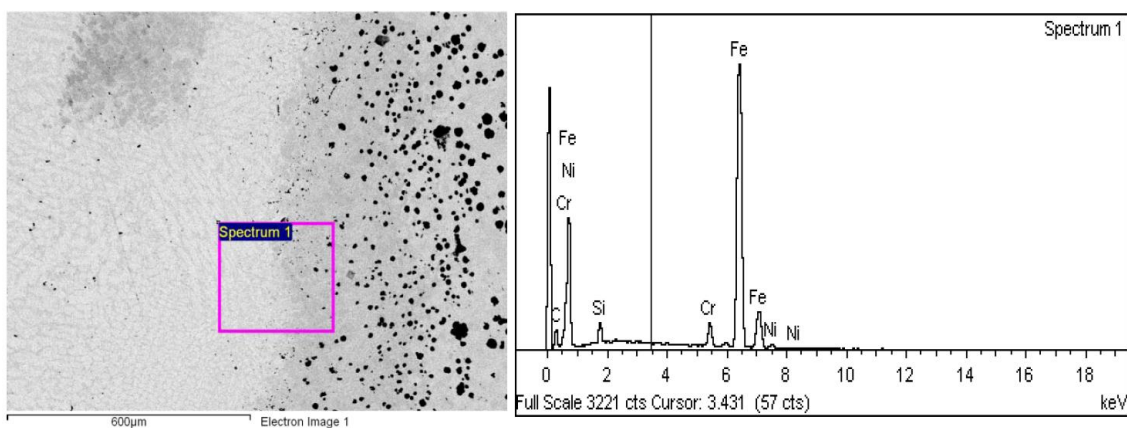


Figure 13. Micrograph and SEM taken at the root weld interface (Inconel 625) with annealing at 900 °C that shows a continuing high Cr level. The hardness level is high but lower than without heat treatment although the structure remains brittle.

5. Conclusions

- Before welding ductile cast iron test plates using an Inconel 625 electrode for the root weld in a single pass and a 97.6% Ni-based electrode for two subsequent filler passes, we preheated the test plates to improve weld fluidity and discourage the formation of brittle structures by favoring penetration and thus preventing fractures from starting. We welded short sections that had been strongly beaten to release residual stress (a process that proved beneficial) and obtained significant mechanical values for resistance and hardness. However, because of the cooling rate, significant values were not obtained for elongation at fracture. By applying a 900 °C annealing treatment and cooling some of the welded test pieces in the furnace, a considerable improvement

was obtained in terms of elongation at fracture, the mechanical values being smaller for breaking strength and elasticity.

- Manual arc welding with an electrode of 97.6% Ni is straightforward, the weld not being excessively fluid and high levels of carbide formation not occurring. Hardness is considerably less than that obtained in the root weld made with an Inconel source rod, although mechanical properties are acceptable and there is greater elongation at fracture.

In the root weld made with an Inconel electrode, the subsequent application of an annealing treatment did not significantly change the initial conditions, and part of the white iron structures and traces of martensitic matrix remained with only small variations in the decrease in hardness and elongation. When the preheat treatment at 350 °C was employed, the fluidity in the pool increased and the mechanical characteristics were higher, and elongation at fracture increased.

Scanning electron microscopy verified the chemical compositions of the structural elements produced and confirmed that annealing treatment after both types of welding produced a greater working capacity in which hardness and tension diminished to enable more ductile fracturing and larger strains. The result is an improvement in the characteristics of the welded unions.

We treated an alloy with 97.6% Ni, which prevented the formation of carbides.

With heat treatment at 900 °C and 97.6% Ni, there is a dissolution of all carbides, forming nodules in ferritic matrix graphite.

Acknowledgments: We would like to give thanks to Language Translators Service of the Languages Department of Universitat Politècnica de València, Spain.

Author Contributions: In this investigation, F.J.C.-C. and M.P.-G. conceived and designed the experiments; F.J.C.-C., R.P.-M., and M.A.P.-P. performed the experiments; F.J.C.-C., R.P.-M., and M.P.-G. analyzed the data; M.A.P.-P. contributed materials/analysis tools; F.J.C.-C. and M.P.-G. wrote the paper.

Conflicts of Interest: The authors declare no conflict of interest.

References

1. Apraiz, J. *Fundiciones*; Editorial Dossat: Madrid, Spain, 1981; pp. 144–145.
2. *Eutectic Castolin: Practice Handbook (Spanish Edition)*; Castolin: Madrid, Spain, 1993.
3. Huke, E.E.; Udin, H. Welding Metallurgy of Nodular Cast Iron. *Weld. J.* **1953**, *32*, 378s–385s.
4. Zhang, X.Y.; Zhou, Z.F.; Zhang, Y.M.; Wu, S.L.; Guan, L.Y. Influence of nickel-iron electrode properties and joint shapes on welded joint strength of pearlitic nodular iron. *Weld. J. Incl. Weld. Res. Suppl.* **1996**, *75*, 280s.
5. Pease, G.R. The Welding of Ductile Iron. *Weld. J.* **1960**, *39*, 1–9.
6. Nonast, R. *Soldado Eléctrico Manual al Arco Metálico*; Gráficas Summa: Madrid, Spain, 1973; p. 84.
7. Fatahalla, N.; Bahi, S.; Hussein, O. Metallurgical parameters, mechanical properties and machinability of ductile cast iron. *J. Mater. Sci.* **1996**, *31*, 5765–5772. [[CrossRef](#)]
8. *Manual de Utilización*; Castolin España: Madrid, Spain, 1993; p. 64.
9. Jeshvaghani, R.A.; Jaberzadeh, M.; Zohdi, H.; Shamanian, M. Microstructural study and wear behavior of ductile iron surface alloyed by Inconel 617. *Mater. Des.* **2014**, *54*, 491–497. [[CrossRef](#)]
10. Steglich, D.; Brocks, W. Micromechanical modelling of the behaviour of ductile materials including particles. *Comput. Mater. Sci.* **1997**, *9*, 7–17. [[CrossRef](#)]
11. Pascual, M.; Cembrero, J.; Salas, F.; Martínez, M.P. Analysis of the weldability of ductile iron. *Mater. Lett.* **2008**, *62*, 1359–1362. [[CrossRef](#)]
12. Cembrero, J.; Pascual, M. Soldabilidad de las fundiciones de grafitoesferoidal. *Rev. Metal.* **1999**, *35*, 392–401. [[CrossRef](#)]
13. El-Banna, E.M.; Nageda, M.S.; El-Saadat, M.M.A. Study of restoration by welding of pearlitic ductile cast iron. *Mater. Lett.* **2000**, *42*, 311–320. [[CrossRef](#)]
14. El-Banna, E.M. Effect of preheat on welding of ductile cast iron. *Mater. Lett.* **1999**, *41*, 20–26. [[CrossRef](#)]
15. Bayati, H.; Elliott, R. Influence of matrix structure on physical properties of an alloyed ductile cast iron. *Mater. Sci. Technol.* **1999**, *15*, 265–277. [[CrossRef](#)]

16. Seferian, D. *Las Soldaduras: Técnica y Control*; Editorial Urmo.: Bilbao, Spain, 1965; pp. 295–299.
17. Kiser, S.D.; Faws, P.E.; Northey, M. Welding Cast Iron: Straightforward. *Can. Weld. Assoc. J.* **2005**, 1–4. Available online: <http://selector.specialmetalswelding.com/publica/cwafall2005.pdf> (accessed on 18 November 2016).
18. Pouranvari, M. On the Weldability of Grey Cast Iron Using Nickel Based Filler Metal. *Mater. Des.* **2010**, *31*, 3253–3258. [[CrossRef](#)]



© 2016 by the authors; licensee MDPI, Basel, Switzerland. This article is an open access article distributed under the terms and conditions of the Creative Commons Attribution (CC-BY) license (<http://creativecommons.org/licenses/by/4.0/>).